Polymer 50 (2009) 4447–4454

Contents lists available at ScienceDirect

Polymer

journal homepage: www.elsevier.com/locate/polymer

Novel synthetic strategy toward shape memory polyurethanes with a well-defined switching temperature

S. D'hollander [a], G. Van Assche [b], B. Van Mele [b], F. Du Prez [a,*]

[a] Department of Organic Chemistry, Polymer Chemistry Research Group, Ghent University, Krijgslaan 281S4-bis, B-9000 Ghent, Belgium
[b] Research Unit Physical Chemistry and Polymer Science (FYSC), Vrije Universiteit Brussel (VUB), Pleinlaan 2, B-1050 Brussels, Belgium

ARTICLE INFO

Article history:
Received 14 April 2009
Received in revised form
23 June 2009
Accepted 10 July 2009
Available online 17 July 2009

Keywords:
Shape memory polyurethane
TPU
Poly(ε-caprolactone)

ABSTRACT

Shape memory polyurethanes (SMPUs) have been synthesised via a novel synthetic methodology, resulting in an improvement of the phase separation in the multi-block structure of the polyurethane and in its shape memory properties. ABA block copolymers based on semi-crystalline poly(ε-caprolactone) and amorphous poly(propylene oxide) (PPO) were used as precursor for the SMPUs. For their synthesis, poly(ε-caprolactone) diols have been converted into isocyanate end-capped prepolymers by using a mixture of 3(4) isocyanato-1-methyl-cyclohexylisocyanate isomers, after which a coupling with low-T_g poly(propylene oxide) oligomers is done. The shape memory polymers are obtained by reaction of the ABA block copolymers with hexamethylenediisocyanate and 1,4-butanediol as chain extender. Using this new strategy, a flexible segment (PPO) was introduced between the hard and the switching segments of the SMPU. For comparison, SMPUs without flexible segment have also been prepared with the conventional synthetic route. DSC, isostrain experiments and cyclic shape memory tests revealed narrower switching temperatures for the SMPUs including a flexible segment.

1. Introduction

Shape memory polymers (SMPs) are smart materials responding to an external stimulus such as temperature [1], magnetic field [2] or electromagnetic radiation [3]. They are defined as materials that have the ability to store a new shape (secondary shape) after deformation and restore to the originally primary shape when an external trigger is applied. Three basic types of shape memory materials exist comprising alloys [4], ceramics [5] and polymers or a combination of them such as in composites [6]. The ceramics and alloys have a different mechanism compared to polymers to restore their original shape but the resulting macroscopic effect is the same. Their mechanism is based on a martensitic transition between two structures [7,8]. The alloys, known for more than 50 years, are used in many applications [9]. During the last decade, the interest for shape memory polymers is growing strongly as a result of their advantages such as light weight, large recovery ability, superior processability and lower cost. Because of their special properties, shape memory polymers have acquired applications in several industrial domains, such as sensors [10], actuators [11], active disassembly [12] and biomedical devices [13].

Among all polymer architectures already reported for shape memory purposes, cross-linked and thermoplastic systems are the most popular comprising semi-interpenetrating polymer networks (semi-IPNs) [14] and ABA structures [15], but also blends have been reported [16]. In the current work, multi-segmented thermoplastic polyurethanes (TPUs) retained our attention because they have the unique ability to change their primary shape and their preparation protocols leave numerous possibilities for adapting their physical properties in a broad window. Because of this, the use of TPUs as shape memory polymers (SMPUs) has already been reported for a number of high-tech applications [17]. In all these cases, *switching* and *permanent* segments are covalently attached during the synthesis. The switching segment mainly determines the transition temperature (T_{trans}) of the SMPU. Heating up the material above this temperature creates an increase in mobility, and as a result of the entropy elasticity the material returns to its primary shape. On the other hand, heating the polymer above the highest transition temperature of the permanent segments destroys the primary shape and creates the ability to change its shape. If T_{trans} is above room temperature, these characteristics turn these SMPUs into the so-called *reversible thermosets* at room temperature, reversible elastomers above T_{trans}, and fluids or polymer melts above the melting point of the permanent segments.

Shape memory behavior requires a sharp transition from the glassy state to rubbery state, a long relaxation time, and a high ratio

* Corresponding author. Tel.: +32 9 264 45 03.
E-mail address: filip.duprez@ugent.be (F. Du Prez).

0032-3861/$ – see front matter © 2009 Elsevier Ltd. All rights reserved.
doi:10.1016/j.polymer.2009.07.021

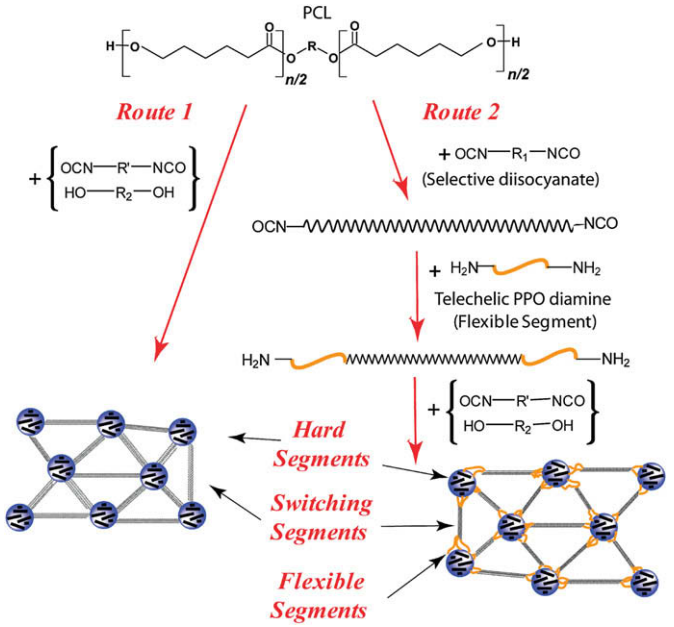

Fig. 1. Scheme of the classical (route 1) and novel synthetic methodology (route 2) for the preparation of SMPUs. The switching segments are drawn in stretched shape for sake of clarity.

of glassy modulus to rubbery modulus (or from semi-crystalline to amorphous state) [18]. The extent of phase separation of the multi-block structure strongly affects these properties and is known to be influenced by parameters such as chemical structure, composition and sequence-length distribution of the hard and switching segments in the segmented copolymer [19–21]. The aim of our research was to adapt the polymer architecture in such a way that the micro-phase separation between the switching and permanent segments is enhanced in an attempt to optimize the shape memory properties.

For comparison reasons, SMPUs were first synthesised via the classical approach (route 1, Fig. 1), which consists of the reaction between semi-crystalline diols with diisocyanates and chain extenders. The drawback of this strategy is that the hard blocks crystallize at higher temperature and hamper the crystallisation of the switching segments, resulting in broader shape memory transitions [22]. Therefore, a novel synthetic strategy was investigated (route 2, Fig. 1) by introducing a short flexible segment between the switching and the permanent segments, which was supposed to provide flexibility for the crystallisation of the switching segments and thus in an improvement of the micro-phase separation between both crystallisable segments and of the shape memory properties.

Polycaprolactone (PCL) has been selected as switching segment. As reported by others [23–26], it is a suitable segment for shape memory purposes due to its semi-crystalline behavior with a melting point around 60 °C and its low glass transition temperature of −60 °C. While linear PCLs show well-defined melting temperatures (T_m) that depend on their number-average molecular weight (M_n), it is also known that the crystallinity is disturbed when these polymers are introduced in a multi-block system resulting in reduced crystallinity and broader melting endotherms [25,26].

2. Experimental

2.1. Materials

All chemicals, unless otherwise noted, were purchased from Sigma–Aldrich. Oligo(ε-caprolactone) diols with M_n values of 6000 and 10 000 g/mol were provided by Solvay Caprolactones and dried overnight in vacuum (120 °C/1 mbar) over P_2O_5. A mixture of 3(4)-isocyanato-1-methyl-cyclohexylisocyanate isomers (IMCI) was kindly donated by DSM (The Netherlands) and was distilled before use. Hexamethylenediisocyanate (HDI) (99%) was purchased from Fluka. 1,4-Butanediol (BDO) (99.9%) is purchased from Aldrich. Poly(propylene glycol)-bis-(2-amino-propyl ether) with an M_n of 400 Da is dried overnight in vacuum over P_2O_5. Ethyl acetate and chloroform (HPLC grade) are freshly distilled over CaH_2 before use. Zirconium (IV) acetylacetonate (>96%) was obtained from Fluka. Dibutyltin dilaurate was kindly donated by Recticel NV (Wetteren, Belgium).

2.2. Characterization

^{1}H NMR spectra were recorded on a Bruker 300 MHz NMR spectrometer in dimethyl sulfoxide-d_6 (DMSO-d_6) or chloroform-d ($CDCl_3$). Polyurethane samples were heated to 80 °C before measurement to ensure the dissolution of the polymer. In another set-up, SEC was performed on three serial mixed-B columns from Polymer Labs at 50 °C, using a refractive detector (2410 Waters). *N*,*N*-Dimethylacetamide containing 0.42 mg/L LiBr was used as mobile phase (flow rate: 1 mL/min), and the system was calibrated with narrow polydisperse poly(methyl methacrylate) (PMMA) standards. Matrix-assisted laser desorption/ionization time-of-flight (MALDI-TOF) spectra were recorded with a PerSeptive

Table 1
Composition of shape memory polyurethanes (route 1).

Entry	M_n PCL (g/mol)	Composition (relative mol ratio)			HS content[a] (wt%)	PCL content[b] (wt%)	M_w[c] (g/mol)	PDI[d]
		HDI	BDO	PCL				
I-1	6000	3.5	2.5	1.0	12	88	112 000	1.98
I-2	6000	5.1	4.1	1.0	17	83	95 000	2.01
I-3	6000	6.0	5.0	1.0	20	80	119 000	1.96
I-4	6000	8.1	7.1	1.0	25	75	121 000	1.97
I-5	6000	10.3	9.3	1.0	30	70	99 000	1.94
I-6	6000	12.9	11.9	1.0	35	65	105 000	1.95
I-7	10 000	5.6	4.6	1.0	12	88	121 000	1.95
I-8	10 000	8.3	7.3	1.0	17	83	115 000	1.92
I-9	10 000	10.0	9.0	1.0	20	80	112 000	2.02
I-10	10 000	13.3	12.3	1.0	25	75	117 000	1.94
I-11	10 000	16.9	15.9	1.0	30	70	108 000	1.98
I-12	10 000	21.2	20.2	1.0	35	65	116 000	1.99

[a] Calculated by dividing the weight of HDI and BDO by the total weight.
[b] Calculated by dividing the weight of PCL by the total weight.
[c] Determined by SEC calibrated with PMMA standards. Solvent: DMA + 0.42 g/L LiBr.
[d] Polydispersity index.

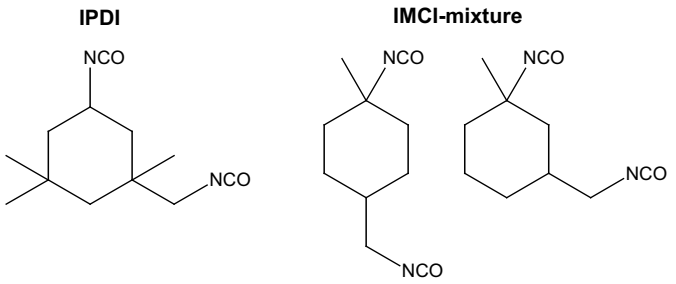

Scheme 1. Structure of the used selective diisocyanates.

Biosystems Voyager DE STR MALDI-TOF spectrometer equipped with 2 m linear and 3 m reflector flight tubes and a 337 nm nitrogen laser (3 ns pulse). All mass spectra were obtained with an accelerating potential of 20 kV in positive ion mode and in linear and/or reflector mode. *trans*-2-[3-(4-*tert*-Butyl-phenyl)-2-methyl-2-propenylidene]malononitrile (BMPM) (20 mg/mL in THF) was used as a matrix, sodium iodide (1 mg/mL) as a cationating agent, and polymer samples were dissolved in THF (2 mg/mL). Analyte solutions were prepared by mixing 10 μL of the matrix, 5 μL of the salt, and 5 μL of the polymer solution. Subsequently, 0.5 μL of this mixture was spotted on the sample plate, and the spots were dried in air at room temperature. A poly(ethylene oxide) standard ($M_n = 2000$ g/mol) was used for calibration. All data were processed using the software Data Explorer (Applied Biosystems). Differential scanning calorimetry (DSC) measurements were performed on a TA instruments Q2000 with LNCS cooling accessory at a heating rate of 10 °C/min. Samples were heated until a temperature of 200 °C and cooled down to −30 °C at a speed of 10 °C/min to erase the thermal history. Isostrain experiments were performed on a dynamic mechanical analyser from TA instruments (DMA 2980) on rectangular films at a heating rate of 1 °C/min. Mechanical and cyclic thermomechanical experiments were performed on a Tinius Olson H10K-T tensile machine with a 100 N load cell. For the cyclic shape memory tests a thermochamber with temperature controller and connected to a liquid nitrogen Dewar is used. The testing cycle was programmed in the Navigator Plus software as described in the literature [27]. Samples were pressed in a two stage press at 200 °C with 100 MPa pressure.

2.3. Synthetic procedures

2.3.1. Synthesis of SMPUs based on poly(ε-caprolactone)

In a two-neck round-bottom flask approximately 5 g PCL is dried overnight and dry ethyl acetate was added (50 wt%). HDI and BDO are added in stoichiometric amounts. After thoroughly mixing, 0.0075 mol% of dibutyltin dilaurate was added. The mixture is injected with a dry syringe between 2 glass plates covered with Teflon foil and separated by a 2 mm silicon rubber. The system is reacted in the oven at 70 °C for 6 h. Afterwards the sample is dried in vacuum at 80 °C for 12 h. The dried samples are pressed prior to analysis.

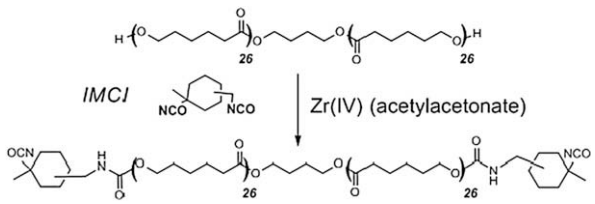

Scheme 2. Synthesis of isocyanate end-capped polycaprolactone.

2.3.2. Synthesis of PPO-b-PCL-b-PPO

In a two-neck round-bottom flask PCL is dried overnight. Under inert atmosphere dry chloroform (250 wt%), zirconium(IV) acetylacetonate (1 mol% per OH group) and 2 equiv. of IMCI are added. The mixture is refluxed at 80 °C for 2 h. After the mixture is cooled down, 20 equiv. (10-fold excess) of poly(propylene glycol)-bis-(2-amino-propyl ether) is added and the mixture is again refluxed for 12 h at 80 °C. The ABA block copolymer is purified by two successive precipitations in cold diethyl ether from chloroform and dried in vacuum prior to analysis (SEC, ^{1}H NMR and MALDI-TOF MS).

2.3.3. Synthesis of SMPUs based on telechelic ABA block copolymers

The synthesis is similar to that of SMPUs based on PCL (2.3.1). In this case, PPO-*b*-PCL-*b*-PPO is used as starting compound instead of pure PCL.

3. Results and discussion

3.1. Synthesis of SMPUs based on PCL

The first part of this work consisted of the synthesis of SMPUs using a classical approach (route 1, Fig. 1). Such SMPUs have been prepared starting from three components: PCL for the switching segment and the combination of BDO and HDI for the permanent

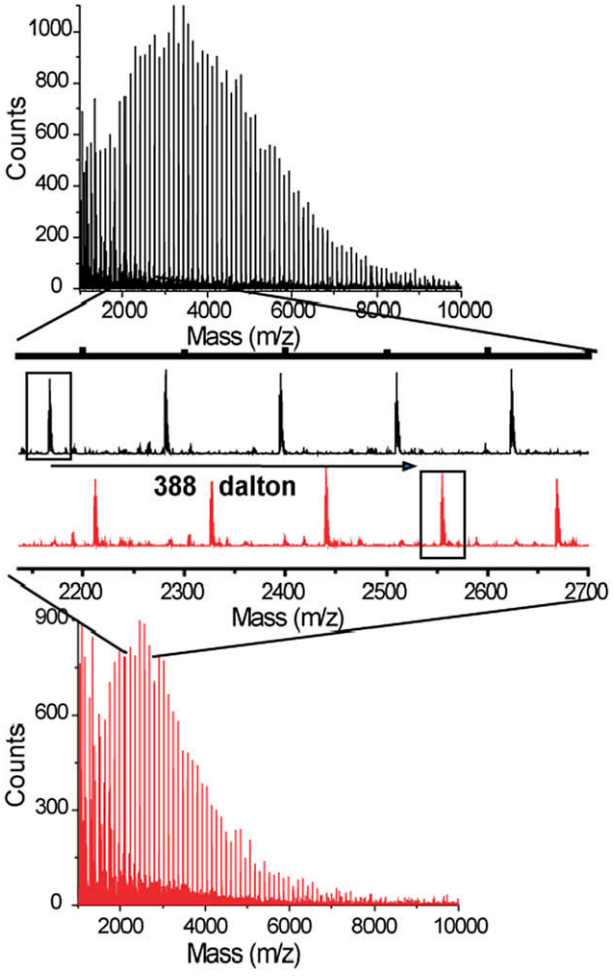

Fig. 2. MALDI-TOF MS analysis of PCL (top) and isocyanate end-capped PCL (bottom), including the magnification of both isotope distributions (middle).

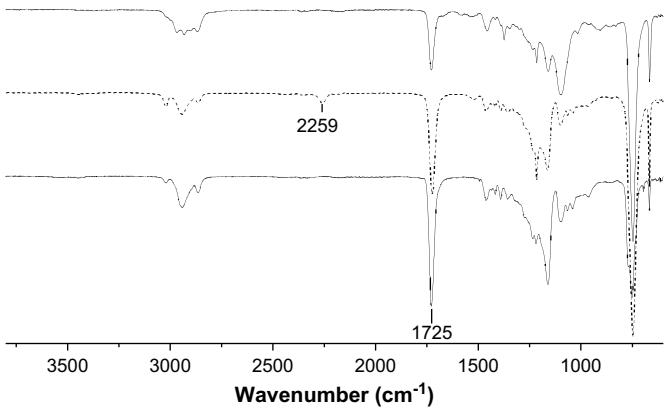

Fig. 3. FTIR spectrum of PCL_{6000} (bottom), IMCI end-capped PCL_{6000} (middle) and ABA block copolymer PPO-*b*-PCL-*b*-PPO (top).

segment (see Experimental Part). PCL with molecular weight of 6000 and 10 000 g/mol was used to evaluate the influence of the length of the switching segment on the shape memory effect. In Table 1 the characteristics of the synthesised SMPUs with different hard segment content are summarized.

The weight average molecular weights of the obtained polymers (PDI around 2) are all in the same range of about 100 000 g/mol, which is sufficient to obtain good film properties for further evaluation of the material properties.

3.2. Synthesis of ABA block copolymers

For the introduction of the flexible segment, a strategy based on the synthesis of a telechelic ABA block copolymer has been chosen. First the two hydroxyl end groups of PCL are converted into isocyanate end groups. Although the most popular and widely used selective diisocyanate is isophorone diisocyanate (IPDI), its selectivity is not high enough to eliminate coupling as described by Van Benthem et al. [28] (Scheme 1).

For that reason, another selective isocyanate has been selected, namely IMCI (2 isomers) having one tertiary and one primary isocyanate group. It has been described earlier [29] that the use of zirconium(IV) acetylacetonate as catalyst results in a reaction with complete regioselectivity, leading to PCL with two tertiary isocyanate end groups (Scheme 2).

The end group modification of PCL was by analogy with literature confirmed by MALDI-TOF MS [30], ^{1}H NMR [31] and FTIR analysis. As the synthesis of the ABA block copolymer is carried out in a one pot process, samples have been taken from the reaction mixture after 2 h to evaluate the isocyanate end capping. ^{1}H NMR spectroscopy proved the full conversion of the hydroxyl end groups. The triplet assigned to the protons next to the hydroxyl group at 3.62 ppm disappears and a new triplet from the two protons next to the isocyanate function appears at 3.03 ppm (see below Fig. 4, H_e).

Comparison of MALDI-TOF MS spectra of PCL before and after end capping with IMCI shows a shift of 388 Da, which can be assigned to the presence of two IMCI molecules per polymer chain (Fig. 2). Besides this clear shift, no extra signals due to coupling are visible. In Fig. 3, the FTIR spectrum before and after end capping is shown. At 1725 cm^{-1} the ester carbonyl stretch of PCL is visible while after end capping the typical asymmetrical N=C=O stretch signal at 2259 cm^{-1} is appearing.

In the next step, the isocyanate end-capped PCL has been converted into ABA bock copolymers by adding a 10-fold excess of low molecular weight, amine-functionalized PPO (400 g/mol) to the end-capped polymer. SEC analysis confirmed that a significant excess is necessary to avoid coupling of the polymers. For example, a clear increase in molecular weight was observed when a 2-fold excess was used. The broad signal at 3.5 ppm in the ^{1}H NMR spectrum of the resulting block copolymers corresponds to

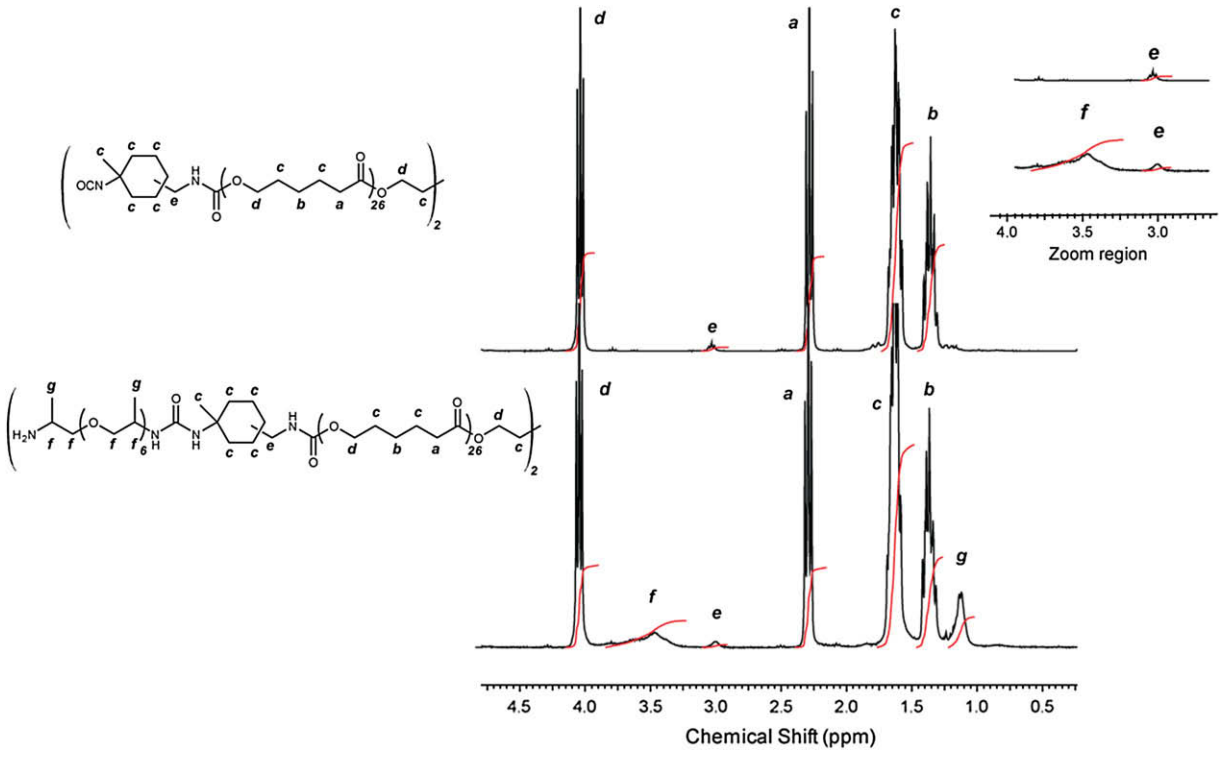

Fig. 4. ^{1}H NMR spectrum (300 MHz, $CDCl_3$) of IMCI end-capped PCL (top) and PPO-*b*-PCL-*b*-PPO (bottom).

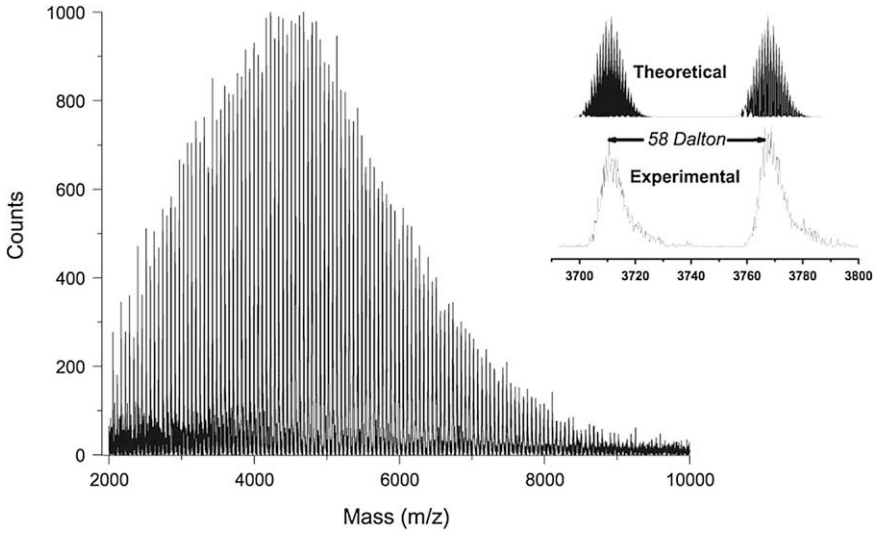

Fig. 5. MALDI-TOF MS spectrum of PPO_{400}-*b*-PCL_{6000}-*b*-PPO_{400}.

the protons of the PPO backbone (Fig. 4). By comparison of the relative integrations of the protons of the PPO backbone (H_f) with those of PCL (H_d), it could be concluded that the conversion of NCO end-capped PCL into PPO-*b*-PCL-*b*-PCL was a quantitative process.

To further confirm the coupling of PCL and PPO segments into an ABA block copolymer, the structure was analysed by MALDI-TOF MS (Fig. 5). Since the molecular weight of the structural unit of PCL (114 Da) is almost twice as high as the one of PPO (58 Da), only one molecular weight distribution can be observed in contrast to the complex MALDI-TOF structures that are usually observed for block copolymers [32].

In the last step of the synthesis, the previously synthesised block copolymers have been used as switching segments for the TPUs. In Table 2, the compositions of the different multi-block copolymers, obtained by the reaction of the amine-functionalized PPO–PCL–PPO with HDI and BDO, are presented. To facilitate comparison between the classical and novel shape memory polymers afterwards, the compositions are chosen in such a way that the hard content is equal to the SMPs synthesised via route 1 (compare entries ending with the same number, e.g. I-4 with II-4). Although the molecular weights are slightly lower than the polymers synthesised via route 1, the material properties for the shape memory tests were not affected (see below).

3.3. Evaluation of the recovery

The shape memory properties have been evaluated with cyclic tensile tests [33] (Fig. 6). In such tests SMPUs are first heated above the switching temperature (step 1) and then stretched (step 2) at elevated temperature. In the next step the materials are cooled down ($T = 20\,^{\circ}C$) (step 3), which results in a decrease of the stress because of crystallisation of the PCL switching segments. During step 4, the sample is reheated without stress and the movement is recorded by the tensile machine. Below the switching temperature, the sample keeps its shape because of the crystallinity of the switching segments. After reaching the PCL melting temperature, the material restores under entropic force.

In the 2-D plot (Fig. 6, right) the quantification of the shape memory effect is shown. Two main parameters define the quality of the shape memory material: strain recovery rate R_r and strain fixity rate R_f [34]. The strain fixity rate (R_f) expresses how well the

Table 2
Composition of shape memory polyurethanes (route 2).

Entry	M_n PCL (g/mol)	Composition (relative mol ratio)			HS content[a] (wt%)	PCL content[b] (wt%)	M_w[c] (g/mol)	PDI[d]
		HDI	BDO	ABA[e]				
II-1	6000	4.2	3.2	1.0	12	73	95 000	1.88
II-2	6000	6.1	5.1	1.0	17	69	72 000	2.09
II-3	6000	7.3	6.3	1.0	20	67	75 000	1.98
II-4	6000	9.6	8.6	1.0	25	63	87 000	1.96
II-5	6000	12.3	11.3	1.0	30	58	91 000	2.04
II-6	6000	15.4	14.4	1.0	35	54	79 000	1.98
II-7	10 000	6.3	5.3	1.0	12	79	89 000	1.93
II-8	10 000	9.3	8.3	1.0	17	74	92 000	1.89
II-9	10 000	11.2	10.2	1.0	20	72	97 000	2.03
II-10	10 000	14.9	13.9	1.0	25	67	101 000	1.91
II-11	10 000	19.0	18.0	1.0	30	63	96 000	1.95
II-12	10 000	23.8	22.8	1.0	35	58	103 000	1.93

[a] Calculated by dividing the weight of HDI and BDO by the total weight.
[b] Calculated by dividing the weight of PCL by the total weight.
[c] Determined by SEC calibrated with PMMA standards. Solvent: DMA + 0.42 g/L LiBr.
[d] Polydispersity index.
[e] ABA = PPO_{400}-*b*-PCL-*b*-PPO_{400}.

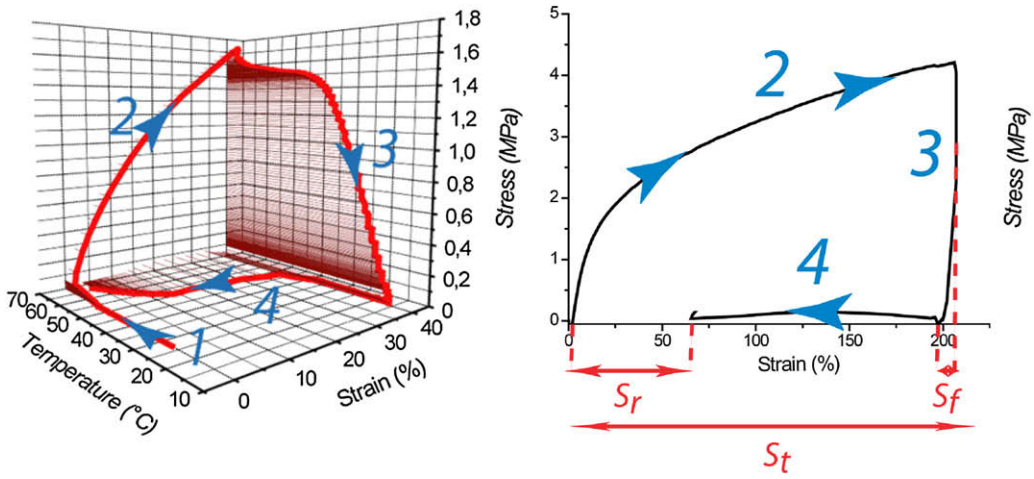

Fig. 6. Cyclic tensile test of entry I-3. Left: 3-D plot (40% strain); Right: 2-D plot (200% strain). (1) Heating. (2) Elongation. (3) Cooling. (4) Recovery (reheating). S_r: Strain recovery failure; S_f: Strain fixity failure; S_t: Total strain.

material can maintain the total strain S_t of the secondary shape after releasing the force on the sample (Equation (1)). The strain recovery rate (R_r) indicates the quality of the restoration of the primary shape after reheating (Equation (2)).

$$R_f = \frac{S_t - S_f}{S_t} \quad (1)$$

$$R_r = \frac{S_t - S_r}{S_t} \quad (2)$$

The results for the SMPUs synthesised via both routes are summarized in Table 3. In the first three experiments, a clear decrease in strain fixity and recovery under increasing strain S_t (from 40 to 200%) is observed as a result of the destruction of hard domains and the shear of polymer chains [22]. This effect diminishes with increasing hard segment content (Exp 3–6). For the shape memory polymers synthesised via route 2 (Exp 7–10) also an increase in R_r with increasing hard segment content is observed. Neither in the strain fixity nor in the strain recovery, a deterioration of the values due to the slightly lower molecular weight of SMPUs, synthesised via route 2 can be observed. On the other hand, an improvement in strain fixity or strain recovery due to the implementation of the flexible segment is not observed. For repeated experiments, the strain fixity and recovery values increased to a high extent. Starting from the second cycle, the strain recovery values approach 99%. Neither the composition nor the flexible segment has a remarkable influence when the experiment is cycled.

Table 3
Strain fixity (R_f) and strain recovery (R_r) values for the first shape memory cycle of SMPUs synthesised via routes 1 and 2.

Experiment	SMPU	% HS[a]	S_t (%)	R_r (%)	R_f (%)
Exp 1	I-3	20	40	90.1	99.1
Exp 2	I-3	20	100	81.2	97.9
Exp 3	I-3	20	200	72.3	96.8
Exp 4	I-4	25	200	75.3	96.3
Exp 5	I-5	30	200	76.5	95.1
Exp 6	I-6	35	200	78.3	96.6
Exp 7	II-9	20	200	73.2	96.3
Exp 8	II-10	25	200	75.2	95.9
Exp 9	II-11	30	200	76.1	95.9
Exp 10	II-12	35	200	77.3	94.8

[a] Calculated by dividing the weight of HDI and BDO by the total weight.

3.4. Evaluation of switching temperature

To evaluate the effect of the flexible segment on the phase separation in the multi-block copolymer, differential scanning calorimetry (DSC) was used. Fig. 7 (upper part) shows the glass transition region of the amorphous fraction, and the melting regions of the switching and the permanent segments of SMPUs

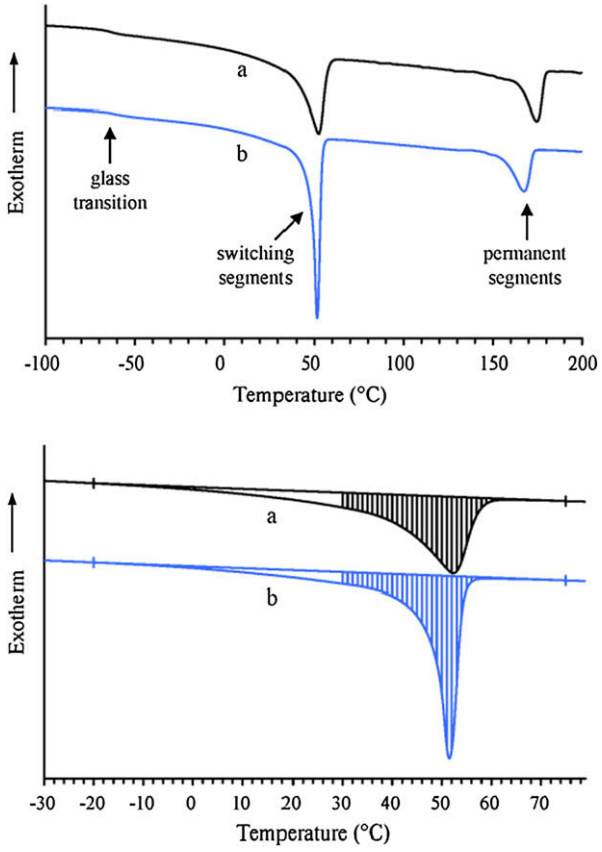

Fig. 7. Upper part: Overlay DSC thermograms with glass transition region and melting region of switching and permanent segments of SMPUs prepared via route 1 (a) (Entry I-11, Table 1) and via route 2 (b) (entry II-11, Table 2); Lower part: The partial integration at 30 °C of the melting peak of the switching segments.

Table 4
Melting enthalpies of PCL in shape memory polymers synthesised via routes 1 and 2.

Experiment	Entry	PCL content (%)	HS content (%)	ΔH_{melt} (J/g)	$\Delta H_{melt.PCL}$[a] (J/g)	25 °C $\Delta H_{melt.PCL\ part}$		30 °C $\Delta H_{melt.PCL\ part}$	
						(J/g)	(%)[b]	(J/g)	(%)[b]
Exp-1	I-2	83.0	17.0	44.2	53.2	44.2	83.0	38.5	72.3
Exp-2	II-2	69.3	17.0	48.8	70.5	65.5	93.0	62.4	88.5
Exp-3	I-4	75.0	25.0	40.4	53.8	42.9	79.7	38.7	71.9
Exp-4	II-4	62.6	25.0	43.7	69.8	64.7	92.7	60.0	86.0
Exp-5	I-5	70.0	30.0	32.1	45.9	35.2	76.8	36.2	78.9
Exp-6	II-5	58.4	30.0	39.5	67.5	61.0	90.3	56.9	84.3
Exp-7	I-8	83.0	17.0	45.5	54.8	49.0	89.5	44.7	81.5
Exp-8	II-8	74.2	17.0	46.2	62.2	59.3	95.3	57.4	92.1
Exp-9	I-10	75.0	25.0	39.8	53.0	45.0	84.8	41.5	78.3
Exp-10	II-10	67.0	25.0	44.9	67.0	60.5	90.2	57.7	86.0
Exp-11	I-11	70.0	30.0	34.7	49.5	45.1	91.0	42.7	86.1
Exp-12	II-11	63.0	30.0	42.0	66.7	63.4	95.1	61.3	92.0

[a] Enthalpy recalculated to the amount PCL present in the sample = ΔH_{melt}/(% PCL content).
[b] % = ($\Delta H_{melt.PCL\ part}/\Delta H_{melt\ PCL}$) × 100.

prepared by routes 1 and 2. The melting endotherm of PCL was compared in the systems with (Fig. 1, route 2) and without PPO flexible segment (Fig. 1, route 1) to evaluate the efficiency of the switching segment at T_{trans}. For SMPUs prepared by route 2 the temperature region of melting is narrower and the melting enthalpy increased (Fig. 7). The partial integration of the melting endotherm, starting around room temperature (e.g. 25 or 30 °C, see arched area in Fig. 7, lower part) and calculated as a percentage of the total enthalpy of melting (% $\Delta H_{melt.PCL\ part}$, Table 4),was used to quantify this effect. This procedure is adequate because it expresses the remaining crystallinity of the switching segment that keeps the material in its secondary shape. Thus, the higher this percentage at a certain temperature, the better the secondary shape is preserved (higher stability) at that specific temperature.

For the different compositions of SMPUs synthesised via routes 1 and 2, all melting enthalpy results are summarized in Table 4. When SMPUs with the same hard segment content are compared, an increase in melting enthalpy can be observed for SMPUs synthesised via route 2. This means that despite the fact that there is a lower amount of PCL (Table 4, PCL content) in the multi-block copolymer, the melting enthalpy is higher because of an increased crystallinity of the switching segments. If the total melting enthalpy values are recalculated corresponding to the effective amount of PCL present in the SMPUs, a clear increase of more than 10 J/g for SMPUs synthesised via route 2 can be observed.

Also when the partial melting enthalpies ($\Delta H_{melt.PCL\ part}$), are considered, the percentages of remaining crystallinity are higher for the SMPUs synthesised via route 2. These values can be related to the stability of the secondary shape. In Table 4 the values for the partial enthalpy at 25 and 30 °C are presented to illustrate the effect of the flexible segment at increasing temperature. When the results of SMPUs with PCL having a molecular weight of 6000 g/mol (Table 4, Exp 1–6) are compared to the ones having a molecular weight of 10 000 g/mol (Exp 7–12), the relative increase in the partial enthalpy for SMPUs with switching segments of lower molecular weight is larger, resulting in a higher stability. For example when the samples with 17% hard segment are compared, the increase in $\Delta H_{melt.PCL}$ is much higher for entry II2 versus I2 (M_n = 6000 g/mol) than for entry II8 versus I8 (M_n = 10 000 g/mol). This can be explained by the fact that the crystallisation of the lower molecular weight switching segments are more hampered by the hard blocks due to the direct coupling of the hard and the switching segments.

To further evaluate the transitions of the shape memory materials, isostrain experiments were performed on a DMA apparatus. The samples were first heated above the transition temperature (70 °C), then stretched and cooled to room temperature to keep them in their secondary shape. While these stretched samples are clamped under isostrain conditions, heating and cooling were successively applied in the DMA apparatus. For the first heating an irregular curve is observed due to clamp effects (not shown in the figure). When the sample is cooled and heated again, this leads respectively to a decrease (Fig. 8, 1) and increase (Fig. 8, 3) of the stress when the shape memory effect takes place. By doing these experiments the stability of the secondary shape as a function of increasing temperature could be measured. When the process was cycled, reproducibility of the effect could be proven (Fig. 8, 4).

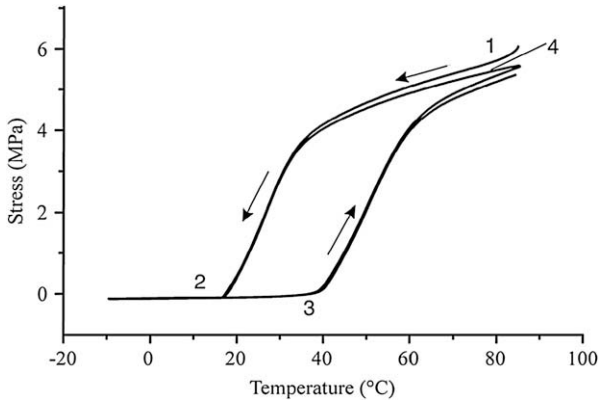

Fig. 8. Isostrain cycling experiment by DMA analysis (Entry II-3): (1) Cooling. (2) Shape fixity temperature. (3) Shape recovery onset. (4) Start of second cycle.

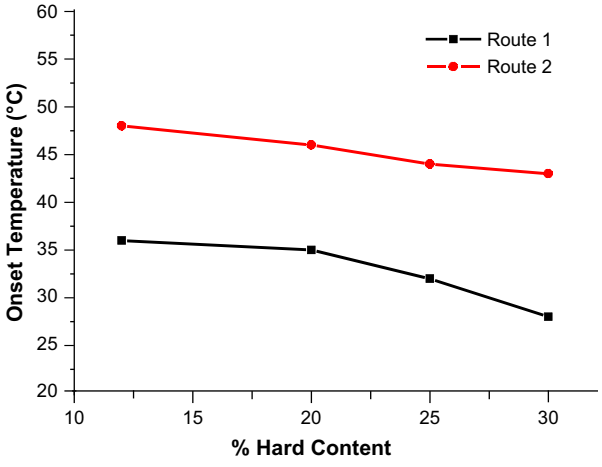

Fig. 9. Onset temperatures from isostrain experiments on SMPUs based on PCL (M_n = 10 000 g/mol) with different hard segment content.

By comparison of both preparation methods, a clear increase in the stability of SMPUs prepared by route 2 could be observed. In Fig. 9, showing isostrain experiments as a function of temperature, the onset of the switching temperatures (Fig. 8, temperature 3) for SMPUs synthesised via both routes as a function of the hard segment content is presented. For each of the tested SMPUs, the incorporation of a flexible segment increases the stability with 10–15 °C. A decrease in the onset temperatures with increasing percentage of hard segment can be observed in 9. Indeed, for an increasing hard segment content, the crystallisation of the switching segments is more hampered. As mentioned before, a less constrained crystallisation of the switching segments determines the stability and the trigger temperature of the shape memory material.

A study on the influence of the flexible segment on the domain formation of the SMPUs, by making use of proton wide line NMR and X-ray scattering techniques, shall be reported in a forthcoming paper.

4. Conclusions

In this paper, two strategies to synthesise polyurethane based shape memory polymers are compared. One route uses a known strategy based on a PCL homopolymer as switching segment while the novel route makes use of switching segments based on PPO-*b*-PCL-*b*-PPO. These ABA block copolymers were successfully synthesised without coupling reactions via a strategy based on the use of a regioselective isocyanate. These block copolymers have been successfully used as precursor for the synthesis of polyurethane based SMPUs. The effect of these flexible segments on the phase separation and the shape memory properties was studied by DSC, isostrain experiments and cyclic mechanical tests. The incorporation of short PPO segments between the switching and the hard segments causes an increase in melting enthalpy and makes the temperature region of melting narrower. When the macroscopic effect of the flexible segment was studied, a better stabilization of the secondary shape was observed, showing the relevance of using flexible spacers between the switching and permanent segments in shape memory polymers.

Acknowledgements

The authors thank the IWT (The Institute for the Promotion of Innovation through Science and Technology in Flanders, Belgium) for a PhD scholarship. The Belgian Program on Interuniversity Attraction Poles initiated by the Belgian State, Prime Minister's office (Program P6/27) and the STIPOMAT ESF-program are acknowledged for financial support.

References

[1] Tobushi H, Hayashi S, Kojima S. JSME Int J Ser I 1992;35(3):296–302.
[2] Mohr R, Kratz K, Weigel T, Lucka-Gabor M, Moneke M, Lendlein A. Proc Natl Acad Sci U S A 2006;103(10):3540–5.
[3] Lendlein A, Jiang HY, Junger O, Langer R. Nature 2005;434(7035):879–82.
[4] Chen H, Kubo H. Curr Opin Solid State Mater Sci 1996;1(3):349–54.
[5] Evans AG. Am Ceram Soc Bull 1979;58(3):338.
[6] Ratna D, Karger-Kocsis J. J Mater Sci 2008;43(1):254–69.
[7] Miyazaki S, Otsuka K. ISIJ Int 1989;29(5):353–77.
[8] Cederstrom J, Vanhumbeeck J. Illrd European symposium on martensitic transformations (ESOMAT 94); 1994. p. 335–41.
[9] Cai W, Meng XL, Zhao LC. Curr Opin Solid State Mater Sci 2005;9(6):296–302.
[10] Kunzelman J, Chung T, Mather PT, Weder C. J Mater Chem 2008;18(10):1082–6.
[11] Monkman GJ. Mechatronics 2000;10(4–5):489–98.
[12] Chiodo JD, Harrison DJ, Billett EH. P I MECH ENG B-J ENG 2001;215(5):733–41.
[13] Lendlein A, Kelch S. Clin Hemorheol Microcirc 2005;32(2):105–16.
[14] Zhang SF, Feng YK, Zhang L, Sun JF, Xu XK, Xu YS. J Polym Sci Polym Chem 2007;45(5):768–75.
[15] VanCaeter P, Goethals EJ, Gancheva V, Velichkova R. Polym Bull 1997;39(5):589–96.
[16] Jeong HM, Ahn BK, Kim BK. Eur Polym J 2001;37(11):2245–52.
[17] Merline JD, Nair CPR, Gouri C, Bandyopadhyay GG, Ninan KN. J Appl Polym Sci 2008;107:4082–92.
[18] Hu J. Shape memory polymers and textiles. Hong Kong: Woodhead Publishing; 2007.
[19] Peebles LH. Macromolecules 1976;9(1):58–61.
[20] Koberstein JT, Galambos AF. Macromolecules 1992;25(21):5618–24.
[21] Hernandez R, Weksler J, Padsalgikar A, Choi T, Angelo E, Lin JS, et al. Macromolecules 2008;41(24):9767–76.
[22] Harper C. Handbook of plastics, elastomers, and composites. McGraw-Hill Professional; 2002.
[23] Li FK, Zhang X, Hou JN, Xu M, Lu XL, Ma DZ, et al. J Appl Polym Sci 1997;64(8):1511–6.
[24] Alteheld A, Feng YK, Kelch S, Lendlein A. Angew Chem Int Ed 2005;44(8):1188–92.
[25] Ping P, Wang WS, Chen XS, Jing XB. Biomacromolecules 2005;6(2):587–92.
[26] Ping P, Wang WS, Chen XS, Jing XB. J Polym Sci Part B Polym Phys 2007;45(5):557–70.
[27] Takahashi T, Hayashi N, Hayashi S. J Appl Polym Sci 1996;60(7):1061–9.
[28] van Benthem RATM, Hofland A, Peerlings HWI, Meijer EW. Prog Org Coat 2003;48(2–4):164–76.
[29] Van Benthem RA, Stanssens DA. WO98/52995; 1998.
[30] Chattopadhyay DK, Raju NP, Vairamani M, Raju K. Prog Org Coat 2008;62(2):117–22.
[31] Prabhakar A, Chattopadhyay DK, Jagadeesh B, Raju K. J Polym Sci Polym Chem 2005;43(6):1196–209.
[32] Montaudo G, Samperi F, Montaudo MS. Prog Polym Sci 2006;31(3):277–357.
[33] Kim BK, Lee SY, Xu M. Polymer 1996;37(26):5781–93.
[34] Lendlein A, Kelch S. Angew Chem Int Ed 2002;41(12):2034–57.